Photo-induced Bending and Buckling of Polymer Sheets

IOP Conf. Series: Materials Science and Engineering **493** (2019) 012029 doi:10.1088/1757-899X/493/1/012029

Photo-induced Bending and Buckling of Polymer Sheets

Jinqiang Wang, Bei Zhang, Pengfu Lei and Ning Dai *

School of Mechanical and Electrical Engineering, Nanjing University of Aeronautics and Astronautics University, Nanjing, China

*Corresponding author e-mail: dai_ning@nuaa.edu.cn

Abstract. Shape-shifting has widespread applications in soft robots and self-assembly structures. To achieve their functionalities, these architectures rely on the spatially bending and buckling to transform the polymer sheets into desired configurations. The goal of this work is to demonstrate that it is possible to tune the shape-shifting behavior through the photo-induced mismatch strain. For the mechanistic understanding, Finite element modeling of thin sheets with different geometry are performed to understand the fundamental mechanics behind the shape transformation behavior. Our experiments with cross-linked polymer samples that change shapes through variation in illumination dose and photo patterns confirm the proposed model predictions. Finally, self-folding structures include flowers, claws, pyramid and saddle are duplicated based on the computational models, indicating the guidelines reported here would be applicable to a diverse array of self-assembly devices.

1. Introduction

The realization of initially flat functional materials capable of autonomous reconfiguration into 3D shapes is an emerging area of research that holds a lot of promise for an unprecedented control over the actuation of function devices. Consequently, researchers look into the nature for inspiring design paradigms. From the wrinkling of our skin[1] to the folding of leaves,[2] biological systems shape themselves for optimal function through shape-shifting across multiple length and time scales. Owing to the continuous exploration in material and manufacturing technique, the fundamental mechanism of shape-shifting have been utilized to produce self-assembly systems where the thin structures demonstrate different shape transformation in response to stimuli such as light, pH, heat, residual stress and electric field.[3-6]As a result, the above-mentioned framework has been applied to achieve functionalities in sensing, medicine, soft robotics, electronics and microfluidics.[5,7-9]

The first important aspect of shape-morphing is the way how shapes change. Within the broad range of stimuli, light provides unique advantages due to their remote activation, spatially control by using photo patterns or light intensity. The most well-know light-motivated shape-shifting strategy is front photoloymerization(FPP),[3,10]which is ubiquitous in lithograpgy, as well as 3D printing, and is thus a pillar of self-assembly fabrication.Without the change of temperature of solvent, and with limited conversion time, FPP can synthesize highly crosslinked polymer networks from liquid resin. Furthermore, FPP is directional and controllable using UV light exposure,which enables multi-level pattering by spatially vaarying photo masks. Due to the nuture of the polymerization process which develops and propagates as a planar wave into the resin, there is a sharp interfacial profile between the cured nerwork and monomer bath. Thus, an obvious mechnical difference exists along the curing deepth,

which induce internal stress gradients eventually. Mechanically, to relax the prestresses, in previous study,[3,11-13] it was demonstrated that the films would undergo complex shape shifting-transformation, where the curvature increased gradually with the irradiation of UV light.

Many theoretical studies on FPP, have resulted in a series of mathematical models to domonstrate the polymerization kinetics and propagation revolution, which are amenable to both mathematical analysis and perdicitive shape-shifting. Xie et al. [14] developed a FPP-based ultrafast printing process of multi-dimensional responsive polymers. Instead of direct printing, their metho relied on physical masks to spatio-selectively define swellability in polymer films. Zhao et al. [3] revealed an intersection of origami art and FPP science, in which 2D light patterns with spatial control over intensity were produced through variation of the grayscale. Despite the process, one drawback of previous contributions is that the geometry of film was ignored. According to Abdullah's work,[12] the behaviors of self-folding structures are often dominated by geometric nonliearities. Stoney[15] made efforts to incorporate geomeric nonlierrities arising from the shape shifting of flat sheets by determing the relationship betweent the isotropic mismatch strains and bending curvatures. While mismatch strain-driven shape-shifting has been studied, a detailed study encompassing the synthesis of FPP and the geometrices of cured films need to be performed.

2. Materials and Experiments

In our approach we use resin consisting of Poly(ethylene glycol) diacrylate (Mn=700, i.e., PEGDA 700) and the dispersant polyethylene glycol (PEG), which are purchased from Sigma-Aldrich (St. Louis, MO, USA). Photoinitiator phenylbis(2,4,6-trimethylbenzoyl) phosphine oxide (Irgacure 819) and photoabsorber Sudan I are purchased from Macklin (Shanghai China). The home-made resin prepare by mixing 90.23 wt% PEGDA 700, 9 wt% dispersant PEG, 0.66 wt% Irgacure 819, and 0.11 wt% Sudan I. To achieve cured flat films, a narrow polymerization zone is desired. Fig.1a shows the whole process schematically. The photo patterns are acquied using available software like AutoCAD. An UV-visible light projector (PRO04500, China, wavelength 405nm) with a projection distance of 182mm is chosen as the light source and its light intensity is measured by an ultraviolet radiometer (UV-A, SKUNUY, China). Fig.1b shows the relation between light intensity and grayscale value.

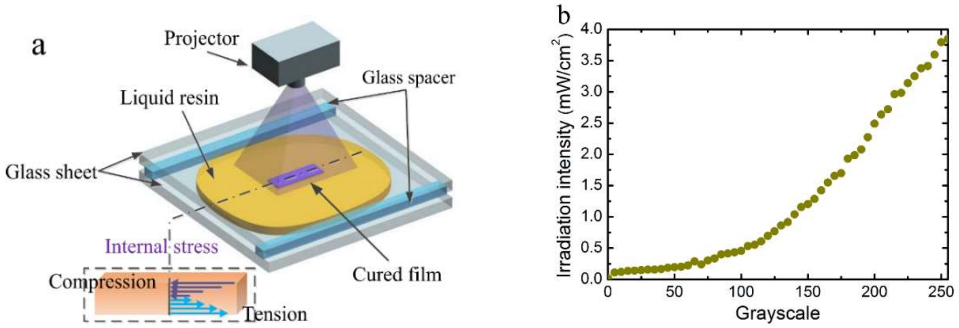

Fig.1 a A schematic presenting the FPP; b Relation between light intensity and grayscale value.

2.1. Mechanical and Photomechanical Revolution

After UV exposure, the revolution of polymerization advances along the direction exposed to light directly. Here, we introduce a minimal FPP model,[10] where a monomer-to-polymer conversion order parameter φ defined $0 \le \varphi \le 1$, from liquid resin to polymerization completion) is considered. In the absence of mass and thermal diffusion, the polymerization conversion profile can be solved to yield:

$$\varphi(z,t) = 1 - \exp[-KI_0 t(-\mu z)] \tag{1}$$

Where z is the direction normal to the illuminated surface (where $z \equiv 0$), t is the UV illumination time, K is a material constant, I_0 is the light intensity at the surface, μ is the attenuation coefficient.

Once the polymerization has commenced, the resin became a solid-liquid coexistence system. Light propagation through a two-component media depth is described by Beer-Lambert law[16] as:

$$\frac{\partial \varphi(z,t)}{\partial z} = -\mu I(z,t) \tag{2}$$

The front position z_f corresponding to the curd depth, which can be solved by defining a critical threshold conversion fraction φ_c equired to form polymer network, where resulting in:

$$z_f = \frac{\ln[KD / \ln(1/1-\varphi_c)]}{\mu} \tag{3}$$

Which is therefore predicted to grow logarithmically with illumination dose $D = It$. To determine the conversion fraction φ_c , FTIR spectra are conducted on the polished surfaces and the conversion profiles at different distances are calculated using Ref.10. According to the result shown in Fig.2a, φ_c is 0.22 in our material system. The curing depth is calculated using Eq.3 is shown in Fig.2b when $K = 0.03 cm^2 mW^{-1} s^{-1}, \mu = 4.25 mm^{-1}$, our measurement of strips cured also support the calculation.

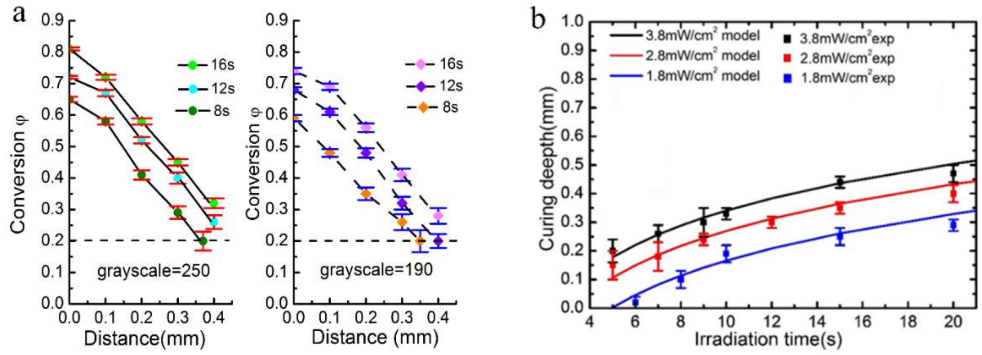

Fig.2 a The extent of conversion across curing depth; b Curing depthes vary with irradiation time.

2.2. Shrinkage-induced Bending Mechanism

After irradiation, the cured film is constrained by the resin, so the out-of-plane rotation is restricted and in-plane stretching dominates. However, significant volume shrinkage strain about 16% occurs after solidification. As is known,[3,5] there is a linear relationship between shrinkage strain Λ and the conversion φ , which can be calculated by $\Lambda = 21.2\varphi$. Once the cured polymer is moved from the substrate, to release the internal stress, the synergy between residual compressive stress and tensile stress drives the film to bend. From the mechanics point of view, the solidified film can be taken as a thin beam. Therefore, although the strain is small, they can bend with large rotation. In addition, the total external force and total external moment applied to the sample is zero and be satisfied:

$$\int_0^{z_f} \sigma dz = \int_0^{z_f} E\varepsilon_t^e dz = 0 \tag{4}$$

$$\int_0^{z_f} z\sigma dz = \int_0^{z_f} zE\varepsilon_t^e dz = 0 \tag{5}$$

Where E is the Young's modulus that varies as $E(\varphi) = 0.19\exp(5.56(\varphi - 0.22)) + 0.32$, ε_t^e is the total elastic strain. After releasing the constraint, the film bends with a curvature κ . The bending results

from the mismatch strain across the depth that arise from the depth-wise gradient in the mechanical properties.

Once proved that volume shrinkage is responsible for large deformation, we modeled and experimentally investigate the deformation forms under different geometries. As such, to calculate the value of κ, we study the simplest case of a slender(i.e. small thickness as compared to length and width) in response to a non-homogenous strain firstly, and a simple Euler-Bernoulli model[11] derived from the composite beam theory is applicable. Hence the radius of bending curvature ρ subject to different conversion degree can be acquired by the equation:

$$\kappa = \frac{1}{\rho} = \frac{\int_0^{z_f} E\varepsilon^s (z-\tilde{z})dz}{\int_0^{z_f} E(z-\tilde{z})dz} \tag{6}$$

Where $\tilde{z}$ is the location of the natural axis computed as follows:

$$\tilde{z} = \frac{\int_0^{z_f} Ezdz}{\int_0^{z_f} Edz} \tag{7}$$

A qualitative understanding of Eq.6 is that numerator above represents the bending moment produced by the differential volume shrinkage, and the denominator characterizes the bending stiffness. During FPP, the bending stiffness increase monotonically with the effective illumination dose while the bending moment possesses a more complex varying trend. Therefore, as shown in Fig.3a, we measured the distribution of Young's modulus and shrinkage strain along the curing thickness. At low irradiation dose, the modulus and strain are small and the bending moment is too weak compared to the bending stiffness to deform the beam, resulting in a large radius of bending curvatures. As the dose increase, there is a dramatic increase of bending moment compared with bending stiffness, thereby causing the beam to bend with a decreasing curvature. However, the decreasing differences in modulus and shrinkage strain cause a reduction of bending moment, which when coupled with the enhancement of bending stiffness lead to an increase in radius of curvatures. The experimental result of rectangle strips cured with different illumination intensity, are shown in Fig.3b, where they yield nearly an identical trend with the simulation based on Eq.6. Thus the simulation model can be used as a predication during photopolymerization process.

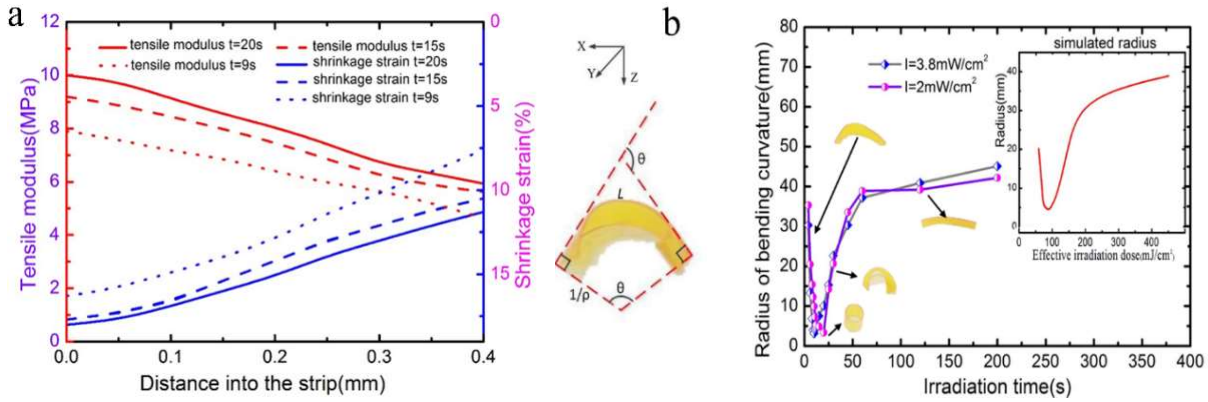

Fig.3 a The distribution of Yong's modulus and shrinkage strain along the curing thickness; b Radius of bending curvature for the beams.

2.3. Simulation of Buckling Deformation

Besides bending, buckling is another activation of shape-shifting.[8] To establish a comprehensive mechanistic understanding of the shape-morphing behavior of polymer films, we had an insight into the deformation principles of a plane geometry. According to previous research, the thin elastic discs practically are NEP (non-Euclidean plates),[17] which satisfy the elastic energy function $E = E_b + E_s$, being a combination of a stretching term and a bending term. According to our experimental observation, the plate-like films experience both bending and stretching due to mismatch strain. This morphing is energetically favorable. At low strains, the combination of out-of-plane bending and in-plane stretching drive the films into quasi-axisymmetric shapes with nonzero Gaussian curvatures. However, the polymerization rate is sublinear with internal stress, which results in an increase of mismatch strain as the irradiation dose enhance. Hence, the plate films bifurcate into approximately singly curved states at critical strains. Although bifurcation of the shape is a universal phenomenon for polymer thin sheets, the curvature could be tuned through illumination dose and initial shapes.

As the goal of is work was to understand the bifurcation of polymer films in FPP, and eventually develop design principles for self-folding structure, we concentrate on the geometric of the films to avoid experimental and computational efforts. We consider a family of regular convex polygonal sheets that belong to the same circumscribing circle (shown in Fig.4a). The polygons approach their circle when the number of edges increase, starting from the triangle and followed by a square. At low mismatch strains, the deformation behavior is almost axisymmetric. However, due to edge effects, the corners and edges will deform in a different manner, resulting in a bifurcation of bending curvature. Since bifurcation need lower stain as the number edges increase, they will approach the critical strain. This trend could be understand by considering the bending energy as an area integral,[17]thus stretching dominates the deformation in smaller integral area (the triangles) while bending competes with stretching aggressively in larger integral area (the circle).

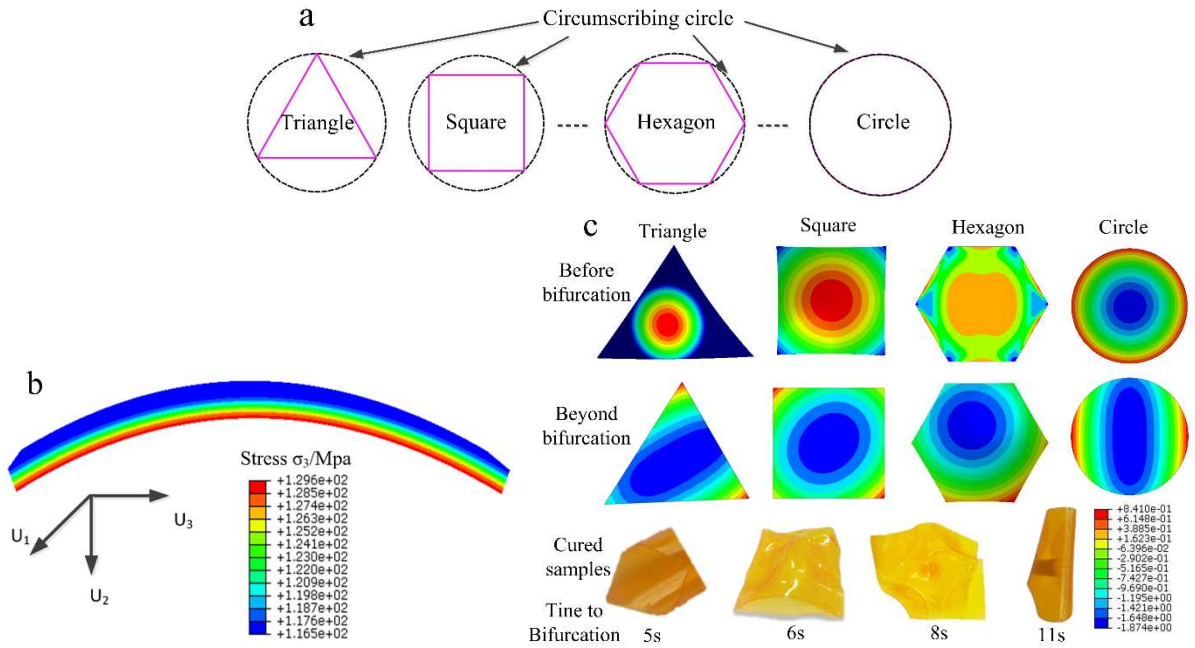

Fig.4 a Regular convex polygons and their circumscribing circles; b FEM simulation of beam; c. FEM of polygons before and beyond bifurcation as well as the experimental results.

To inspect the bifurcation behavior and identify the design principles for generating self-folding configurations, we validate the finite method using ABAQUS. In our model, the shape transformation of plate is analyzed as a hypothetical thermal expansion mismatch problem. Similar strategy has been

widely applied to strain-driven shape morphing in diverse material systems.[8,18] In our simulation, the polymer film is simplified as bilayer (active layer shows a larger expansion than the passive layer when the temperature increase). In the computations, four-node general purpose shell elements are applied. We fix the centroidal nodes of the films while restricting their rigid body movements to replicate the shape-morphing behavior. The active layer is assigned a hypothetical positive thermal expansion coefficient with respect to the passive one. All the finite element calculations were performed using a Young's modulus of 4MPa and a Poisson's ratio of 0.39. We firstly perform the simulation on a slender shown in Fig.4b and the result not only show stress gradient along the curing depth but also demonstrate an obvious bending deformation. Then, a family of polymer films with different geometries were cured under the same illumination intensity until the bifurcation occurs. Fig.4c shows the simulation result using our FEM model and the bifurcation shapes in our experiment. The time to bifurcation was recorded, and the result confirmed that triangles take less time to bifurcation and followed by squares, hexagons and circles.

3. Design Scheme of Self-folding Structures

According Fig.4c, before bifurcation, the sheets will bend with two similar curvature along two orthogonal directions. Beyond bifurcation, doubly curved regions near the edges and corners occur,[18] combining with the cylindrical bending, the flat sheets trend to buckling (the double curvatures gradually vanish, and turn out to be a major axis curvature and a minor axis curvature). This happens due to the energy variations is minute. At low mismatch strains, the sheets remain mostly planar and restrict out-of-plane deformation. The increase of mismatch strains will eventually enhance out-of-plane displacement and rotation and hence the bending curvature increases. The geometry effects on curvature-mismatch stain relationship is shown Fig.5a. To remove the dependence of calculation result on specific units, the simulation quantities are non-dimensionalized. As shown, changes in the number of edges is responsible for the location of bifurcation, and bifurcation is preferred for circles at lower mismatch strain. This fact, coupled with revolution of FPP which the internal stress increase with the illumination dose, resulted in an effective design scheme (Fig.5b) to generate self-folding architectures.

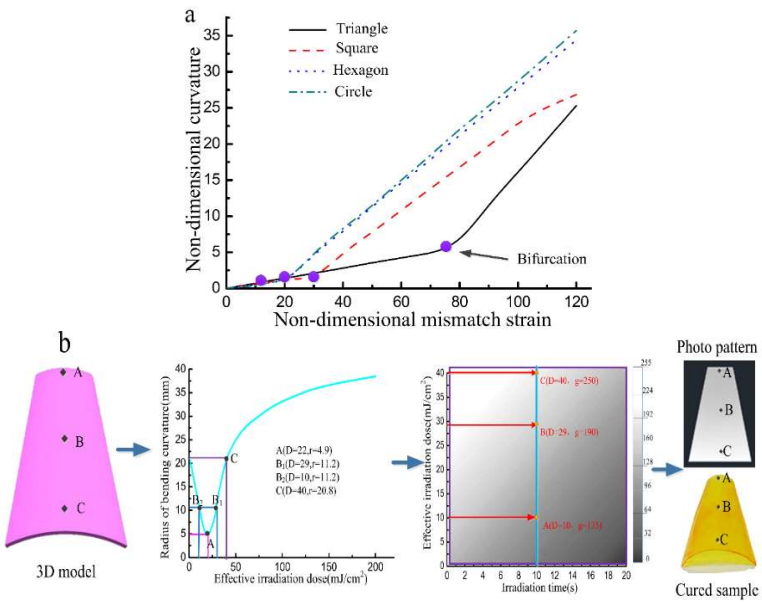

Fig.5 a The geometries effects on bifurcation; b Design scheme of self-folding structures via FPP.

Firstly, the curvature of a 3D model at different locations is acquired through measurement. Since we have built the relation shown in Fig.3b, the irradiation dose is settled based on the radius of bending curvature. In this case, the grayscale value of the projected images are determined with a settled

illumination time. For example, A,B,C are three random dots on the laminate with different curvature ($r_A = 135, r_B = 11.2, r_C = 20.8$), the grayscale value were acquired when the illumination time was 10s($g_A = 135, g_B = 190, g_C = 250$). Similarly, the rest grayscale of the structure were found in the same way. Consequently, we created an analogous structure using FPP. It is very interesting that the existence of holes can also program the bending direction. By introducing holes (circle, ellipse, square and rhombus) in the center of a 40×40mm square, we observe that the folding of thin films with and without holes are different (Fig.6a). In fact, apart from bending along one of the orthogonal axis, bending is expected to occur along diagonal. In fact, the total strain energy will decrease for an increasing size of holes. The experiments confirm that the folding of thin sheets is accelerated by the existence of holes, whose mismatch strain is larger than the flat films. Thus, it demonstrates the possibility of producing more lightweight self-folding structures effectively. The design principles described so far could be used to achieve more smart self-folding structures through FPP. Here, some examples of this idea is presented in Fig.6b-d where a saddle, a hollowed-out octahedron, a claw and a biomimetic flower are shown with different photo patterns.

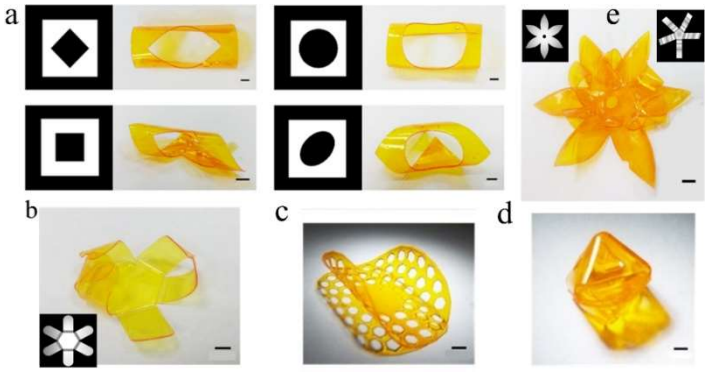

Fig.6 a. Squares with holes will bend into different shapes; b-d Self-folding structures cured by FPP.(6b) Claw;(6c) Saddle;(6d) Octahedron;(6e) Flower.

4. Conclusion

In this paper, we firstly demonstrate a well-controlled patterning approach for photocurable resin based on the characteristic of FPP. Motivated by the revolution of FPP, the internal stress along the curing depth is investigated. Experimentally, we observed that illumination of one side of the slender gradually curled the film bending toward the newly cured layer. To inspect the influence of geometries on the shape-shifting, we replace the complex process of buckling induced by mismatch strain by a simple thermal expansion driven shape morphing of linear elastic material. This approach allow us to achieve the general predictions of the bifurcation of curvature without excessive computational costs and experimental efforts. Other effective methods to tune the shape-shifting including reducing the number of edges or adding holes in the sheets are also proposed. Finally, in the light of our experimental outcome, self-folding structures were created according their curvatures.

Acknowledgments

This work was financially supported by Six talent peaks project in Jiangsu Province, China (No. GDZB-034), the Natural Science Foundation of Jiangsu Province, China (No. BK20161487), Jiangsu Province science and technology support plan project, China (No.BE2016010-4, BE2018010-2, BE2016763), Jiangsu province achievements transformation project (No.BA2016106), Foundation of Graduate Innovation Center in NUAA (kfjj20170523) fund.

References

[1] Ionov L. Biomimetic 3D self-assembling biomicroconstructs by spontaneous deformation of thin

polymer films[J]. Journal of Materials Chemistry, 2012, 22(37): 19366-19375.
[2] Elbaum R, Zaltzman L, Burgert I, et al. The role of wheat awns in the seed dispersal unit[J]. Science, 2007, 316(5826): 884-886.
[3] Zhao Z, Wu J, Mu X, et al. Origami by frontal photopolymerization[J]. Science Advances, 2017, 3(4): e1602326.
[4] Tolley M T, Felton S M, Miyashita S, et al. Self-folding origami: shape memory composites activated by uniform heating[J]. Smart Materials and Structures, 2014, 23(9): 094006.
[5] Pezzulla M, Shillig S A, Nardinocchi P, et al. Morphing of geometric composites via residual swelling[J]. Soft Matter, 2015, 11(29): 5812-5820.
[6] Zhao Z, Wu J, Mu X, et al. Desolvation induced origami of photocurable polymers by digit light processing[J]. Macromolecular rapid communications, 2017, 38(13): 1600625.
[7] Jamal M, Zarafshar A M, Gracias D H. Differentially photo-crosslinked polymers enable self-assembling microfluidics[J]. Nature communications, 2011, 2: 527.
[8] Abdullah A M, Li X, Braun P V, et al. Self-Folded Gripper-Like Architectures from Stimuli-Responsive Bilayers[J]. Advanced Materials, 2018: 1801669.
[9] Taccola S, Greco F, Sinibaldi E, et al. Toward a new generation of electrically controllable hygromorphic soft actuators[J]. Advanced Materials, 2015, 27(10): 1668-1675.
[10] Vitale A, Hennessy M G, Matar O K, et al. A unified approach for patterning via frontal photopolymerization[J]. Advanced Materials, 2015, 27(40): 6118-6124.
[11] Glugla D J, Alim M D, Byars K D, et al. Rigid Origami via Optical Programming and Deferred Self-Folding of a Two-Stage Photopolymer[J]. ACS applied materials & interfaces, 2016, 8(43): 29658-29667.
[12] Abdullah A M, Braun P V, Hsia K J. Bifurcation of self-folded polygonal bilayers[J]. Applied Physics Letters, 2017, 111(10): 104101.
[13] Holmes D P, Roché M, Sinha T, et al. Bending and twisting of soft materials by non-homogenous swelling[J]. Soft Matter, 2011, 7(11): 5188-5193.
[14] Huang L, Jiang R, Wu J, et al. Ultrafast digital printing toward 4D shape changing materials[J]. Advanced Materials, 2017, 29(7).
[15] Stoney G G. The tension of metallic films deposited by electrolysis[J]. Proc. R. Soc. Lond. A, 1909, 82(553): 172-175.
[16] Cabral J T, Douglas J F. Propagating waves of network formation induced by light[J]. Polymer, 2005, 46(12): 4230-4241.
[17] Sharon E, Efrati E. The mechanics of non-Euclidean plates[J]. Soft Matter, 2010, 6(22): 5693-5704.
[18] Alben S, Balakrisnan B, Smela E. Edge effects determine the direction of bilayer bending[J]. Nano letters, 2011, 11(6):2280-2285.